Controlled Precipitation Polymerization of Phthalimidomethyloxirane in Cationic Isomerization Ring-Opening Manner

Shigeyoshi Kanoh,* Tomonari Nishimura, Yasuhiro Mitta, Akihiko Ueyama, and Masatoshi Motoi

Department of Industrial Chemistry, Faculty of Engineering, Kanazawa University, Kodatsuno, Kanazawa 920-8667, Japan

Toshiyuki Tanaka

Department of Pharmacognosy, Gifu Pharmaceutical University, Mitahora-higashi, Gifu 502-8585, Japan

Kenji Kano

Graduate School of Agriculture, Kyoto University, Sakyo-ku, Kyoto 606-8502, Japan

Received April 3, 2001

ABSTRACT: The cationic polymerization of phthalimidomethyloxirane (**1**) with methylaluminum bis(2,6-di-*tert*-butyl-4-methylphenoxide) (MAD) afforded polyether (**2**) or polyacetal (**3**) depending on temperature. Acetalic linkages in the main chain of **3** were formed via isomerization ring opening involving the intramolecular nucleophilic attack of the imide−carbonyl group at the growing end. The polymerization system in toluene at 25 °C became heterogeneous during the polymerization, but the resulting **3** nevertheless had a narrow molecular weight distribution and a degree of polymerization nearly equal to the feed ratio of **1** to MAD. This is the first example of a precipitation polymerization in which the growth to nearly uniform chain lengths was controlled over a very narrow molecular weight range by the physical solubility equilibrium of growing species between solution and precipitates, similar to chemical equilibria between reactive growing ends and dormant covalent species.

Introduction

Developing living polymerization capable of affording polymers with controlled chain architectures has been one of the most challenging fields in synthetic polymer chemistry. Many successes, especially in living chain-growth polymerizations, are ascribed primarily to the development of new initiating systems; the initiator or initiating system should react exclusively with a polymerizable functional group in the monomer at a much faster rate than propagation, and the resulting growing species should be sufficiently stable that no chain-breaking reactions such as chain-transfer reaction or termination take place during the polymerization. Recent strategies for the control of chain-growth polymerization utilize chemical equilibria with growing ends, i.e., the reversible and rapid interchanges between reactive growing ends and dormant covalent species, with the latter predominating. This concept is most likely to become a common key to control almost all possible chain-growth mechanisms, and many examples now appear in the literature for anionic, cationic, group-transfer, coordination, metathesis, and radical polymerizations.[1]

As a conceptual extension to the precise control of polymerization via dormant species, we herein report the controlled precipitation polymerization of phthalimidomethyloxirane (**1**) via the physical solubility equilibrium of the growing species. This new type of polymerization is a cationic isomerization ring-opening polymerization involving the intramolecular nucleophilic attack of the imide−carbonyl group at the growing end. Controlled ring-opening polymerizations of oxiranes have so far been limited to systems polymerizing anionically,[2] or cationically through an activated-monomer mechanism.[3]

Experimental Section

Materials. Boron trifluoride etherate (BF_3OEt_2; Tokyo Kasei Kogyo; >98%) and trimethylsilyl trifluoromethanesulfonate (Aldlich; 99%) were purified by fractional distillation under reduced pressure in a nitrogen atmosphere. Methylaluminum bis(2,6-di-*tert*-butyl-4-methylphenoxide) (MAD) was prepared from trimethylaluminum (Kanto Chemical; 0.98 mol L^{-1} in hexane) and 2,6-di-*tert*-butyl-4-methylphenol (Kanto Chemical; >98%) in anhydrous hexane according to Aida's method[4] and purified by recrystallized from toluene−hexane under nitrogen; 60% yield. The initiator solutions were prepared by dissolving the purified Lewis acids in anhydrous toluene (0.43 mol L^{-1}). Anhydrous triethylamine (Et_3N; Nacalai Tesque; 99%) and anhydrous solvents such as dichloromethane (CH_2Cl_2; Nacalai Tesque; 99%), chlorobenzene (PhCl; Nacalai Tesque; 99%), and toluene (Nakarai Tesque; 99.5%) were purified by conventional methods and distilled under dry nitrogen before use.

Measurements. Size-exclusion chromatography (SEC) was performed on a Shimadzu LC-10A high-speed liquid chromatography system equipped with a differential refractometer, using THF as eluent with a flow rate of 1.0 mL min^{-1} at room temperature; two polystyrene-gel columns with maximum porosities of 7×10^4 and 5×10^3 were connected in series. The molecular weight calibration curve was obtained using standard polystyrenes. Infrared spectra were recorded on JASCO model FT/IR-3 and A-202 infrared spectrometers. ^1H and ^{13}C NMR spectra were measured in $CDCl_3$ using TMS as an internal standard on JEOL JNM GX-400 NMR and JEOL JNM FX-100S spectrometers. Matrix-assisted laser desorption ionization time-of-flight mass (MALDI−TOF−MS) analysis was performed on a PerSeptive Biosystems Voyager-DE RP, equipped with 1.3-m linear and 2.0-m reflection flight tubes

10.1021/ma010577g CCC: $22.00
Published on Web 01/03/2002

as well as a 337-nm nitrogen laser (pulse width, 3 ns). The experiment was done using no salt additive at an accelerating potential of 20 kV. A mixture of angiotensin I (human; MW = 1296.5; Sigma) and adrenocorticotropic hormone (fragment 7-38; MW = 3659.2; Sigma) was used for the calibration of the mass scale. Sample solutions were prepared by dissolving a polymer (2.6 mg mL^{-1}) and dithranol (5.6 mg mL^{-1}; Aldrich) in THF. Immediately after 1.0 mL of the polymer solution and 2.0 mL of the matrix solution were mixed together in a glass vial, 2.0 μL portions of the mixed solution were deposited with a calibrated pipet (Eppendorf) onto the dimples of a sample plate and gently dried under air at room temperature. The plate was inserted into the apparatus under high vacuum (ca. 10^{-6} Pa).

Preparation of 2-Oxiranylmethylisoindole-1,3-dione (1). The oxirane phthalimide (**1**) was prepared from epichlorohydrin (45.0 mL, 0.574 mol) and potassium phthalimide (13.9 g, 75.1 mmol) under refluxing for 5 h, according to a literature method:[5] yield 92%; colorless needles; mp 98−99 °C (acetone−Et_2O); ^{1}H NMR δ 7.87, 7.74 (each dd, J_1 = 5.4 Hz, J_2 = 2.9 Hz, each 2H, carbonyl *m*- and *o*-H_{Ar}), 3.97, 3.87 (each dd, J_1 = 14.7 Hz, J_2 = 4.9 Hz, each 1H, NCH_2), 3.24 (m, 1H, OCH), 2.81 (t-like, J = 4.5 Hz, 1H, *trans*-OCH_2 to CH_2N), 2.69 ppm (dd, J_1 = 4.9 Hz, J_2 = 2.4 Hz, 1H, *cis*-OCH_2 to CH_2N); ^{13}C NMR δ 167.9 (C═O), 134.1 (carbonyl *m*-C_{Ar}), 131.9 (carbonyl *ipso*-C_{Ar}), 123.4 (carbonyl *o*-C_{Ar}), 49.0 (OCH), 46.1 (OCH_2), 39.6 ppm (NCH_2); IR (KBr) 1770, 1723, 1706 ($\nu_{C=O\ imide}$), 1399 (ν_{C-N}), 963, 790 cm^{-1} (ν_{C-O}); HRMS found, *m/e* 203.0594 (calcd for $C_{11}H_9NO_3$, *m/e* 203.0583). Anal. Calcd for $C_{11}H_9NO_3$: C, 65.02; H, 4.46; N, 6.89. Found: C, 65.10; H, 4.34; N, 6.87.

Polymerization of 1 with MAD. Typically, a 10-mL tube, equipped with a three-way stopcock, containing **1** (0.25 g, 1.2 mmol) was repeatedly evacuated and filled with dry nitrogen. Anhydrous toluene (3.0 mL) was added to the tube, and the monomer was dissolved at 25 °C. A toluene solution of MAD (0.43 mol L^{-1}, 0.14 mL, 0.061 mmol) was charged by a syringe in a nitrogen stream, and then the resulting solution was allowed to stand at this temperature. After the polymerization was quenched with anhydrous Et_3N (0.1 mL), volatile materials were evaporated to dryness. A small amount of the residue was subjected to ^{1}H NMR and SEC analyses to determine the product ratio and average molecular weights (M_n and M_w) of the produced polymer, respectively. For instance, the polymerization at 25 °C for 70 h resulted in 73% conversion of **1**, and $M_{n\,SEC}$ of **3** = 2.87×10^3 (M_w/M_n = 1.13): the theoretical number-average molecular weight ($M_{n\,calc}$) of **3** was estimated to be 2.98×10^3 according to $M_{n\,calc} = [\mathbf{1}]_0/[MAD]_0 \times$ MW of **1** (203) × % conversion/100 + FW of H and HO ends (18). The crude polymer, if necessary, was purified by reprecipitation from a concentrated $CHCl_3$ solution with diethyl ether.

Poly{oxy[1-(isoindole-1,3-dione-2-ylmethyl)ethylene]} (2). ^{1}H NMR: δ 7.71 (s-like, 2H, carbonyl *o*-H_{Ar}), 7.60 (s-like, 2H, carbonyl *m*-H_{Ar}), 4.0−3.2 ppm (m, 5H, OCH, OCH_2, and NCH_2). ^{13}C NMR: δ 168.0 (C═O), 133.6 (carbonyl *m*-C_{Ar}), 132.3 (carbonyl *ipso*-C_{Ar}), 123.1 (carbonyl *o*-C_{Ar}), 73−69 (OCH_2 and OCH), 42−38 ppm (NCH_2). IR (KBr): 3450 (m; ν_{OH}), 1770, 1721 ($\nu_{C=O\ imide}$), 1395 (ν_{C-N}), 1118−1046 cm^{-1} (ν_{C-O}).

Poly[oxy(2,3-dihydro-9b*H*-oxazolo[2,3-*a*]isoindol-5-one-9*b*,2-diyl)methylene] (3). ^{1}H NMR: δ 7.9−7.4 (m, 4H, H_{Ar}), 4.6−3.9 (m, 2H, NCH_2), 3.9−3.0 ppm (m, 3H, OCH_2 and OCH). ^{13}C NMR: δ 164.8 (C═O), 141.0 (carbonyl *ipso*-C_{Ar}), 134.0 (acetal *ipso*-C_{Ar}), 133.3 (carbonyl *p*-C_{Ar}), 131.3 (acetal *o*-C_{Ar}), 124.1 (acetal *p*-C_{Ar}), 121.9 (carbonyl *o*-C_{Ar}), 105.7 (acetal-C), 64.3 (OCH), 63.9 (OCH_2), 40.3 ppm (NCH_2). IR (KBr): 3450 (w; ν_{OH}), 1770 (vw; $\nu_{C=O\ imide}$), 1720 ($\nu_{C=O\ lactam}$), 1397 (ν_{C-N}), 1115−978 cm^{-1} (ν_{C-O}).

Monomer-Addition Polymerization. The monomer-addition polymerization was similarly carried out in a centrifuge tube equipped with a glass stopcock at 25 °C. The heterogeneous reaction mixture obtained in 2.5 h was separated into the supernatant solution and the precipitate by centrifugation under nitrogen at 25 °C. An aliquot of each part was taken out and treated with anhydrous Et_3N, and then each part was analyzed by ^{1}H NMR and SEC. The conversion of **1** in the supernatant solution was determined to be 19%, and the soluble part was obtained in 78 wt % after evaporation. From these data, the total conversion of **1** was deduced to be 41%. The $M_{n\,SEC}$ values of soluble and insoluble **3** were 1.72×10^3 (M_w/M_n = 1.13) and 1.78×10^3 (M_w/M_n = 1.12), respectively. The precipitates were used for the second-stage polymerization before complete removal of the slightly remaining solvent. A toluene solution of **1** (0.25 g in 3.14 mL) was added to the tube containing the toluene-wet precipitates immediately after centrifugal separation. The second-stage polymerization was continued for additional 5 h at 25 °C, to give homoblock **3** having $M_{n\,SEC} = 2.58 \times 10^3$ (M_w/M_n = 1.10) in 30% yield based on the first feed of **1** (0.25 g).

Similarly, two polymerizations of **1** with 2.5 mol % of MAD at 25 °C were carried out in toluene for 5 h and in toluene−CH_2Cl_2 (4:1 v/v) for 24 h, and the resulting precipitate parts were separated by centrifugation under nitrogen at 25 °C: $M_{n\,SEC} = 2.26 \times 10^3$ (M_w/M_n = 1.12) for toluene-soluble **3** and 3.64×10^3 (M_w/M_n = 1.18) for toluene−CH_2Cl_2-soluble **3**. About half of a solution of **1** (0.25 g) in toluene−CH_2Cl_2 (4:1 v/v, 3.14 mL) was added to each precipitate part immediately after centrifugal separation, and then the resulting suspensions were mixed together. The second-stage polymerization was continued for additional 24 h at 25 °C, to give **3** showing a unimodal SEC curve: $M_{n\,SEC} = 3.68 \times 10^3$ (M_w/M_n = 1.21).

***p-tert*-Butylphenoxyl End-Capped 3.** A polymer sample of **3** for the end capping[6] was prepared in the polymerization of **1** (0.25 g, 1.2 mmol) with MAD (5 mol %) in toluene (3.0 mL) at 25 °C for 4 h. SEC analysis of an aliquot of the polymerization mixture showed $M_{n\,SEC} = 1.84 \times 10^3$ (M_w/M_n = 1.11). The $M_{n\,calc}$ was presumed to be certainly 1.90×10^3 based on the 46% conversion of **1** in another polymerization under the same conditions. Immediately after the polymerization, a solution of sodium *p-tert*-butylphenoxide (ca. 0.1 mol L^{-1}, 2.5 mL, 0.25 mmol) in anhydrous THF distilled from Na−benzophenone was added to the remaining polymerization mixture, and the homogeneous mixture was stirred at 25 °C for 12 h under a nitrogen atmosphere. The residue obtained by evaporation was dissolved in $CHCl_3$, and repeated precipitation with Et_2O gave *p-tert*-butylphenoxyl end-capped **3**. The IR spectrum of the resulting polymer (cast film) showed two weak absorption bands at 3400 (ν_{OH}) and 1770 ($\nu_{C=O\ imide}$) cm^{-1}, suggesting that the initiating end is a hydroxyl group and the terminating end is a ring-opened ether unit carrying a phthalimide group and a phenoxyl cap, as shown in Scheme 3 (vide infra). The number-average degree of polymerization ($\overline{DP}_{NMR}$) was estimated to be 9.07 from the peak area ratio of the total aromatic protons in the lactam and imide units (7.9−7.4 ppm) to the *tert*-butyl protons (1.24 ppm). Thus, $M_{n\,NMR}$ of **3** before end capping, i.e., **3** having a hydroxyl end in place of a *p-tert*-butylphenoxyl one, was estimated to be 1.86×10^3 according to $M_{n\,NMR} = \overline{DP}_{NMR} \times$ MW of **1** (203) + FW of H and OH ends (18).

Hydrolysis of 3. Hydrolysis of **3** (0.1 g) was carried out in THF (5 mL) containing a few drops of 1 mol L^{-1} hydrochloric acid for 12 h at room temperature, and evaporation almost quantitatively gave crude 2-(2,3-dihydroxypropyl)isoindole-1,3-dione (**4**), which was recrystallized from CH_2Cl_2−hexane to afford pure **4**: colorless needles; mp 106−107 °C; ^{1}H NMR δ 7.87, 7.74 (each dd, J_1 = 5.4 Hz, J_2 = 3.2 Hz, each 2H, carbonyl *o*- and *m*-H_{Ar}), 3.99 (sept-like, J = 5.0 Hz, 1H, OCH), 3.88 (dd, J_1 = 14.4 Hz, J_2 = 5.9 Hz, 2H, NCH_2), 3.64 (ddd, J_1 = 12.7 Hz, J_2 = 6.4 Hz, J_3 = 4.6 Hz, 2H, OCH_2), 2.91 (d, J = 5.9 Hz, 1H, CHO*H*), 2.62 ppm (t, J = 6.4 Hz, 1H, CH_2OH); ^{13}C NMR δ 169.0 (C═O), 134.3 (carbonyl *m*-C_{Ar}), 131.8 (carbonyl *ipso*-C_{Ar}), 123.6 (carbonyl *o*-C_{Ar}), 70.3 (OCH), 63.8 (OCH_2), 40.5 ppm (NCH_2); IR (KBr) 3340 (ν_{OH}), 1772, 1723, 1716 ($\nu_{C=O\ imide}$), 1394 (ν_{C-N}), 1087 cm^{-1} (ν_{C-O}); HRMS found, *m/e* 222.0757 (MH^+) (calcd for $C_{11}H_{11}NO_4 + H^+$, *m/e* 222.0767). Anal. Calcd for $C_{11}H_{11}NO_4$: C, 59.73; H, 5.01; N, 6.33. Found: C, 59.75; H, 4.91; N, 6.32.

Isomerization of *N*-Oxiranylmethylbenzamide (6). Benzoyl chloride (10.0 mL, 86.5 mmol) was slowly added to a solution of allylamine (5.19 g, 90.8 mmol) and Et_3N (24.0 mL,

Scheme 1

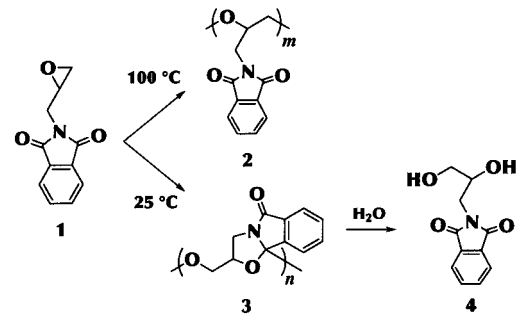

Scheme 2[a]

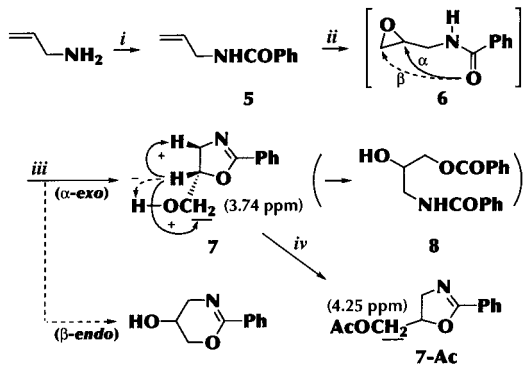

[a] (i) PhCOCl and Et_3N in $CHCl_3$. (ii) *m*CPBA in AcOEt. (iii) H^+ (*m*-chlorobenzoic acid produced in situ). The solid and broken arrows in **7** denote plus and minus NOE, respectively, on irradiating the 5-methine proton of **7**. (iv) Ac_2O and Et_3N in $CHCl_3$.

172 mmol) in $CHCl_3$ (50 mL) at 0 °C, and the mixture was stirred overnight at room temperature. Extractive workup followed by distillation gave *N*-allylbenzamide (**5**: 13.7 g, 84.8 mmol) in 98% yield.

m-Chloroperoxybenzoic acid (*m*CPBA, 3.14 g, 18.2 mmol) was added by potions to a solution of **5** (1.47 g, 8.65 mmol) in ethyl acetate (50 mL), and the resulting solution was stirred at room temperature for 96 h. Extractive workup and chromatographic purification on alumina using ethyl acetate: hexane = 1:2 (v/v) gave (2-phenyl-4,5-dihydro-1,3-oxazol-5-yl)methanol (**7**) (0.339 g, 1.92 mmol) and 3-benzoylamino-2-hydroxypropyl benzoate (**8**) (0.779 g, 2.85 mmol) in 22 and 33% yields, respectively (Scheme 2). However, the ^{1}H NMR spectrum of the above extract revealed that no **8** was included. It was inferred that partial hydrolysis of **7** followed by acyl-transfer to form **8** happened during the chromatographic manipulation.

To confirm the structure of **7** more precisely, it was converted to the acetate (**7-Ac**). Acetic anhydride (0.16 mL, 1.7 mmol) was added to a $CHCl_3$ (3 mL) solution of **7** (151 mg, 0.853 mmol) and Et_3N (0.47 mL, 3.4 mmol) at 0 °C. After stirring for 3 h at room temperature, direct distillation from the reaction mixture afforded **7-Ac** (0.162 g, 0.740 mmol) in 87% yield.

7: colorless liquid; bp 140−160 °C (1 mmHg); ^{1}H NMR δ 7.91 (d-like, J = 8.1 Hz, 2H, *o*-H_{Ph}), 7.46 (t-like, J = 7.3 Hz, 1H, *p*-H_{Ph}), 7.37 (t-like, J = 7.6 Hz, 2H, *m*-H_{Ph}), 4.81−4.74 (m, 1H, OCH), 4.04 (dd, J_1 = 14.6 Hz, J_2 = 9.8 Hz, 1H, NCH_2), 3.81 (dd, J_1 = 15.1 Hz, J_2 = 8.3 Hz, 1H, NCH_2), 3.79 (dd, J_1 = 12.0 Hz, J_2 = 3.7 Hz, 1H, OCH_2), 3.68 (dd, J_1 = 12.2 Hz, J_2 = 5.4 Hz, 1H, OCH_2), 3.56 ppm (br s, 1H, OH); ^{13}C NMR δ 164.2 (imidate-C), 131.4 (*p*-C_{Ph}), 128.3 (*m*-C_{Ph}), 128.1 (*o*-C_{Ph}), 127.3 (*ipso*-C_{Ph}), 80.2, (OCH), 63.8 (OCH_2), 56.1 ppm (NCH_2); IR (KBr) 3200 (ν_{OH}), 1640 cm^{-1} ($\nu_{C=N}$); HRMS found, *m*/*e* 177.0791 (calcd for $C_{10}H_{11}NO_2$, *m*/*e* 177.0790).

7-Ac: colorless liquid; bp 90−110 °C (1 mmHg); ^{1}H NMR δ 7.94 (d-like, J = 8.1 Hz, 2H, *o*-H_{Ph}), 7.48 (t-like, J = 7.0 Hz, 1H, *p*-H_{Ph}), 7.41 (t-like, J = 7.3 Hz, 2H, *m*-H_{Ph}), 4.92−4.87 (m, 1H, OCH), 4.32 (dd, J_1 = 12.0 Hz, J_2 = 3.7 Hz, 1H, OCH_2), 4.19 (dd, J_1 = 12.7 Hz, J_2 = 5.6 Hz, 1H, OCH_2), 4.15 (dd, J_1 = 15.1 Hz, J_2 = 10.3 Hz, 1H, NCH_2), 3.82 (dd, J_1 = 14.7 Hz, J_2 = 7.3 Hz, 1H, NCH_2), 2.09 ppm (s, 3H, CH_3); ^{13}C NMR δ 170.7 (C=O), 163.9 (imidate-C), 131.4 (*p*-C_{Ph}), 128.3 (*m*-C_{Ph}), 128.1 (*o*-C_{Ph}), 127.3 (*ipso*-C_{Ph}), 76.9, (OCH), 65.1 (OCH_2), 56.9 (NCH_2), 20.7 ppm (CH_3); IR (KBr) 1742 ($\nu_{C=O}$), 1644 ($\nu_{C=N}$), 1235 cm^{-1} (ν_{C-O}); HRMS found, *m*/*e* 219.0910 (calcd for $C_{12}H_{13}NO_3$, *m*/*e* 219.0896).

8: colorless liquid; bp 200−230 °C (1 mmHg); ^{1}H NMR ($CDCl_3$−D_2O) δ 8.05 (d-like, J = 8.5 Hz, 2H, *o*-H_{PhCOO}), 7.80 (d-like, J = 5.4 Hz, 2H, *o*-H_{PhCONH}), 7.6−7.3 (m, 6H, *m*- and *p*-$H_{PhCOO\ and\ PhCONH}$), 6.9 (br s, 1H, NH), 4.5−4.0 (m, 2H, OCH_2), 4.0−3.3 ppm (m, 3H, OCH and NCH_2); IR (KBr) 3280 (ν_{OH} and ν_{NH}), 1720 ($\nu_{C=O\ ester}$), 1640 cm^{-1} ($\nu_{C=O\ amide}$).

Results and Discussion

Cationic Polymerization of 1. The cationic polymerization of **1** was investigated using a sterically hindered Lewis acid, methylaluminum bis(2,6-di-*tert*-butyl-4-methylphenoxide) (MAD). The results are summarized in Table 1. Spectroscopic analyses of the products by IR, ^{1}H and ^{13}C NMR, and MALDI−TOF−MS revealed that two kinds of polymers were formed depending on the reaction temperature, as shown in Scheme 1. The IR spectra are most indicative of the different structures. The imide-type carbonyl stretching bands at 1770 and 1720 cm^{-1} in Figure 1A indicate that product **2** is a ring-opening polyether having phthalimide pendant groups, as in the case of common substituted epoxides. This structure was reasonably supported by the ^{1}H and ^{13}C NMR data as well. Evidence that the other product is a polyacetal (**3**) includes the amide-type carbonyl stretching band at 1721 cm^{-1}, the acetal C−O−C stretching bands around 1120−980 cm^{-1} (Figure 1B), the ^{13}C NMR signal at 105.7 ppm characteristic of a quaternary acetal carbon (Figure 2), and the MS ion peaks separated by 203 mass units equal to the formula weight of **1** (Figure 3).[7] Indeed, **3** readily underwent hydrolytic degradation with dilute hydrochloric acid to give 2-(2,3-dihydroxypropyl)isoindole-1,3-dione (**4**) almost quantitatively (Scheme 1). In contrast, **2** composed of open ether linkages was relatively stable under the same conditions.

Acetalic linkages in the main chain of **3** should be formed by intramolecular cyclization during the polymerization process. Five- and six-membered ring structures are possible because the nucleophilic attack of the imide−carbonyl group can occur at either the electrophilic α- or β-carbon in the oxirane ring.[8] However, overlap of the OCH and OCH_2 signals in the ^{1}H and ^{13}C NMR spectra of **3** made spectroscopic interpretation difficult (Figure 2). Thus, we used the acid-catalyzed isomerization of *N*-oxiranylmethylbenzamide (**6**) as a model reaction for the intramolecular carbonyl attack in the cationic polymerization of **1**, since it was found that a similar isomerization of *sec*-amide-substituted oxetanes is not accompanied by cationic polymerization.[9] Oxidation of *N*-allylbenzamide (**5**) with *m*-chloroperoxybenzoic acid (*m*CPBA) yielded 2-phenyl-5-hydroxymethyl-4,5-dihydrooxazole (**7**) instead of the desired epoxide (**6**), as outlined in Scheme 2. The epoxidation of **5** was evidently followed by the acid-catalyzed isomerization of intermediate **6** with the in situ produced *m*-chlorobenzoic acid. The precise ring structure of **7** was confirmed from the NOE differential spectrum under irradiation of the C5-methine proton and from the large carbonyl deshielding observed for the OCH_2 protons of acetylated **7-Ac**. Consequently, this pattern of α-exo

Table 1. Cationic Precipitation Polymerization of 1 with MAD[a]

					polymer			
run	solvent[b]	temp (°C)	time (h)	convn (%)[c]	struct[d]	$M_{n\,SEC}$[e] ($\times 10^{-3}$)	$M_{n\,calc}$[f] ($\times 10^{-3}$)	M_w/M_n[e]
1	T[g]	0	264	48	**3**	2.60	1.98	1.11
2[h]	T	25	1.5	34	**3**	1.34	1.39	1.12
3	T	25	4	46	**3**	1.84[i]	1.90	1.11
4	T	25	70	73	**3**	2.87	2.98	1.13
5[j]	T	25	70	100	**3**	2.87	2.82	1.12
6[h]	T	80	48	92	**2** + **3**	1.89	3.76	1.43
7[h]	T	100	48	100	**2**	1.71	4.08	1.63
8[k]	T:D = 4:1	25	96	100	**3**	5.03	5.09	1.15
9[h]	T:D = 1:1	25	168	100	**3**	4.64	4.08	1.72

[a] Conditions: 0.25 g of **1** (1.2 mmol), 0.14 mL of MAD in toluene (0.43 mol L^{-1}, 0.061 mmol, 5.0 mol %). [b] Solvent 3.0 mL. T: toluene. D: CH_2Cl_2. [c] Determined by ^1H NMR. [d] Determined by IR. [e] Estimated by SEC (polystyrene standards). [f] $M_{n\,calc} = [\mathbf{1}]_0/[MAD]_0 \times$ MW of **1** $\times$ % conversion/100 + FW of H and HO ends (18). [g] Toluene 6.0 mL. [h] Homogeneous. [i] $\overline{DP}_{NMR}$ of *p-tert*-buthylphenoxyl end-capped **3** = 9.07. $M_{n\,NMR}$ of **3** before end capping was estimated to be 1.90×10^3 according to $\overline{DP}_{NMR} \times$ MW of **1** (203) + FW of H and HO ends (18). [j] 7.2 mol % of MAD. [k] 4.0 mol % of MAD.

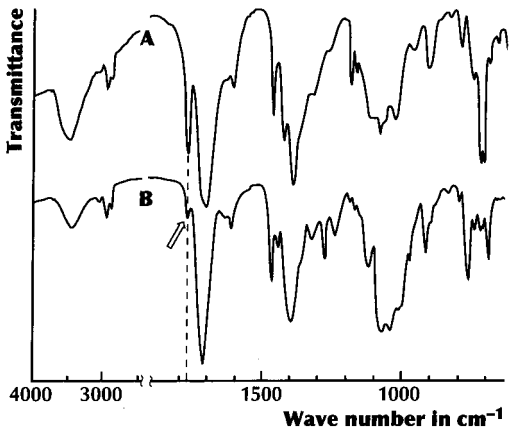

Figure 1. IR spectra of **2** (A) and **3** (B) (cast film on a KBr plate).

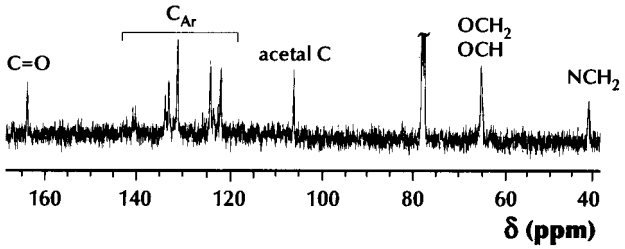

Figure 2. ^{13}C NMR spectrum of **3** in $CDCl_3$.

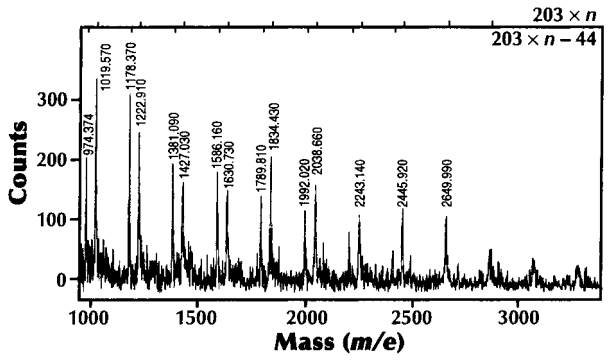

Figure 3. MALDI−TOF−MS spectrum of **3** ($M_{n\,SEC} = 2.77 \times 10^3$, $M_w/M_n = 1.12$).

cyclization strongly supports formation of the five-membered 4,5-dihydrooxazole rings in the polymerization process giving **3**.

IR spectra of the two polymers showed weak to moderate OH stretching bands, and furthermore **3** showed a very weak phthalimide-type shoulder band at 1770 cm^{-1} (Figure 1). These characteristic bands are assignable to the terminal groups of each polymer. The plausible structures of **2** and **3**, including both extremities, are proposed in Scheme 3, based on the hydrolytic termination of the growing polymer ends (vide infra).

Scheme 3

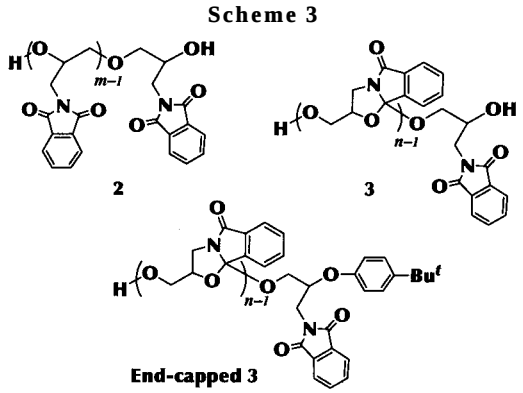

Table 1 shows that the polymerization temperature was a crucial factor for determining the structure of polymer backbone; the products at 25 °C or below were **3** (run nos. 1−5), whereas those above 100 °C were **2** (run nos. 6 and 7). The cationic polymerization of a four-membered oxetane analogue also followed to similar temperature dependence.[8a] Phthalimidomethyl-substituted oxetane first isomerized to a [2.2.2]bicyclic acetal, which polymerized by either a single or a double ring opening to yield the corresponding polyacetal or polyether, respectively. In contrast to the monomer-isomerization mechanism for the oxetane, however, there is no evidence that **1** is converted into a more strained [2.2.1]bicyclic acetal prior to polymerization.

Precipitation Polymerization. Polymerization in toluene at 25 °C gave **3** with narrow molecular weight distributions ($M_w/M_n = 1.10-1.15$) irrespective of precipitation of the product (run nos. 3−5). Figure 4 shows the time−conversion curve in the precipitation polymerization with 5 mol % of MAD and the changes of the M_n and M_w/M_n of **3** produced. The plot of the $M_{n\,SEC}$ has a linear correlation with the conversion throughout the polymerization, regardless of whether the system was homogeneous or heterogeneous. Furthermore, the $M_{n\,SEC}$ agrees well both with the $M_{n\,calc}$ estimated assuming the formation of one polymer per MAD molecule and with the $M_{n\,NMR}$ estimated from *p-tert*-butylphenoxyl end-capped **3**[6] (run no. 3). These results are tentatively suggestive of a living polymerization, although precipi-

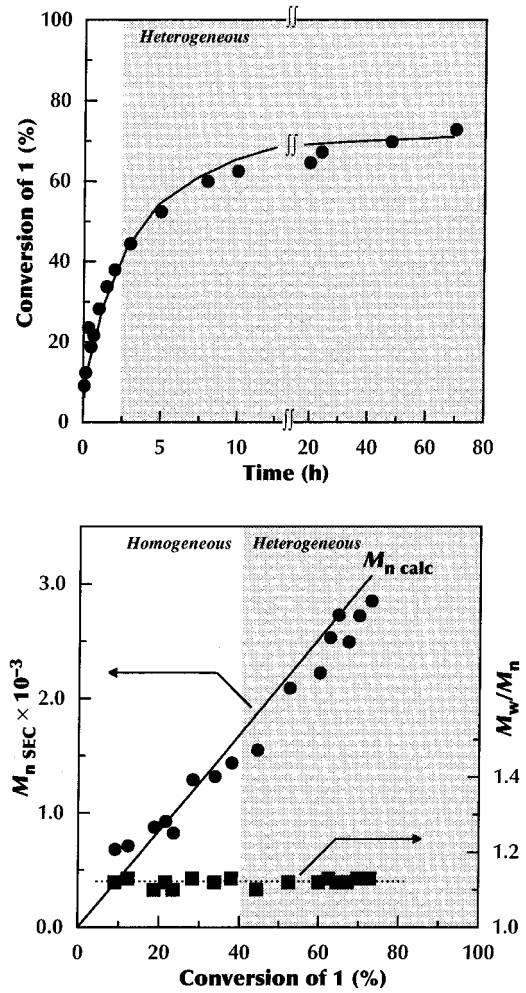

Figure 4. Plots of time−conversion (top) and polymer molecular weight data (bottom) for the precipitation polymerization of **1** with MAD (5 mol %) in toluene at 25 °C. The solid curve indicates the calculated conversion of **1** according to eqs 1 and 3 with $k_p = 2.32 \times 10^{-3}$ mol^{-1} L s^{-1}, whereas the diagonal solid line indicates the calculated $M_{n\,calc}$ assuming the formation of one living polymer per MAD molecule.

tation of polymer is generally believed to spoil the living nature of a polymerization. As seemingly opposed to the living nature, however, the increase of the polymer yield ceased completely near 70% conversion, leaving unreacted **1** (Figure 4). This always occurred when the $M_{n\,SEC}$ reached ca. 2.80×10^3, irrespective of the initial concentration of **1**, and the feed ratio of MAD to **1** (unless the ratio is more than ca. 7 mol %). Similarly, precipitates of **3** always began to appear after the $M_{n\,SEC}$ exceeded ca. 1.60×10^3. This strongly suggests that the solubility of **3** in toluene depends on its own M_n. Thus, quantitative conversion of **1** was achieved in the polymerization with MAD (run no. 5) only when $[\mathbf{1}]_0/[\mathrm{MAD}]_0$ did not exceed 13.7 ($M_{n\,calc}$ not exceeding 2.80×10^3).

The heterogeneous polymerization mixture was separated into the supernatant solution and the precipitate by centrifugation under a nitrogen atmosphere. As compared in Figure 5 (A and B), the SEC curves of **3** in the respective parts showed no difference in M_n except for slight broadening of curve B from soluble **3**. When a toluene solution of **1** was added immediately after centrifugal separation to the precipitate part which was still wet with toluene,[10] the polymerization started again in a heterogeneous state to give a higher-molecular-weight **3** showing a unimodal SEC curve (Figure 5C).

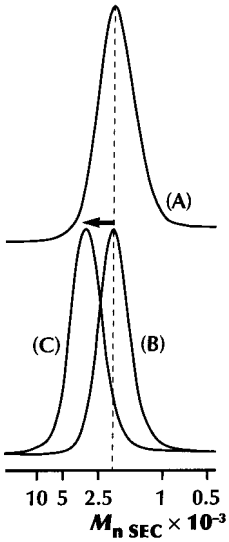

Figure 5. SEC profiles in the monomer-addition polymerization starting with the precipitates of living **3**, which were obtained with MAD (5 mol %) in toluene at 25 °C. The supernatant solution (A: $M_{n\,SEC} = 1.72 \times 10^3$, $M_w/M_n = 1.13$), and the precipitates (B: $M_{n\,SEC} = 1.78 \times 10^3$, $M_w/M_n = 1.12$) in the first stage for 2.5 h. Homoblock **3** (C: $M_{n\,SEC} = 2.58 \times 10^3$, $M_w/M_n = 1.10$) in the second stage for additional 5 h.

Increasing of M_n indicates that the toluene-insoluble **3** is potentially a living species by virtue of the solubility equilibrium with toluene-soluble **3**. In addition, two precipitates from the different polymerizations with different conversions were mixed together, and the monomer-addition polymerization with this mixed system resulted in converging of two separated SEC peaks. This observation indicates that the polymer chains with different length apparently grow with different rates only because of different times spent in insoluble state.

The precipitation polymerization of **1** can be expressed by the following scheme, which includes a solubility equilibrium of the growing species ($\underline{\mathrm{P}^*_n}$: n = number-average degree of polymerization, $\overline{\mathrm{DP}}$) between solution (s) and precipitate (p):

$$\mathrm{I} + \mathrm{M} \xrightarrow{k_i} \mathrm{P}^*_1(\mathrm{s}) \quad \text{initiation}$$

$$\mathrm{P}^*_n(\mathrm{s}) + \mathrm{M} \xrightarrow{k_p} \mathrm{P}^*_{n+1}(\mathrm{s}) \quad \text{propagation}$$

$$\mathrm{P}^*_n(\mathrm{s}) \xrightarrow{K_{(n)}} \mathrm{P}^*_n(\mathrm{p}) \quad \text{solubility of propagating species}$$

It should be stressed that the solubility equilibrium has to be established fast in comparison to the propagation reaction in order to get dormant/living phenomenon.

Assuming rapid initiation ($k_i \gg k_p$)[11] and considering our initial condition ($[\mathrm{M}]_0/[\mathrm{I}]_0 = 20$), the second-order kinetic expression for the homogeneous propagation state ($[\mathrm{P}^*(\mathrm{s})] = [\mathrm{I}]_0$ at $1 \le n \le 7$) can be solved as the following analytical form[12]

$$k_p t = \frac{1}{[\mathrm{I}]_0} \ln\left(\frac{19}{20 - n}\right) \equiv F_{\mathrm{homo}}(n) \qquad (1)$$

where $F_{\mathrm{homo}}(n)$ refers to a function of n in a homogeneous state.

On the other hand, under the heterogeneous conditions ($1.60 \times 10^3 < M_n \le 2.80 \times 10^3$), the solubility of **3** in toluene decreases with increasing M_n or $\overline{\mathrm{DP}} = n$. As

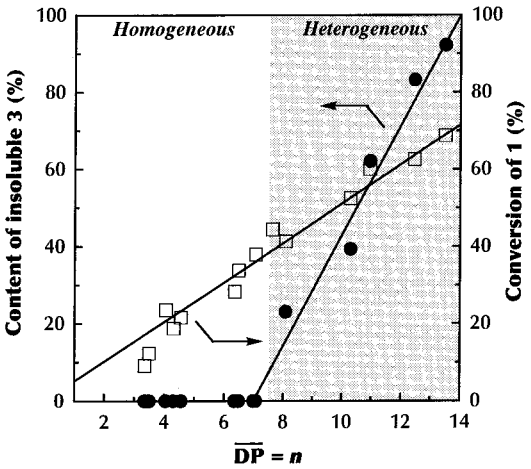

Figure 6. Content of toluene-insoluble **3** in the polymerization of **1** with MAD (5 mol %) in toluene at 25 °C.

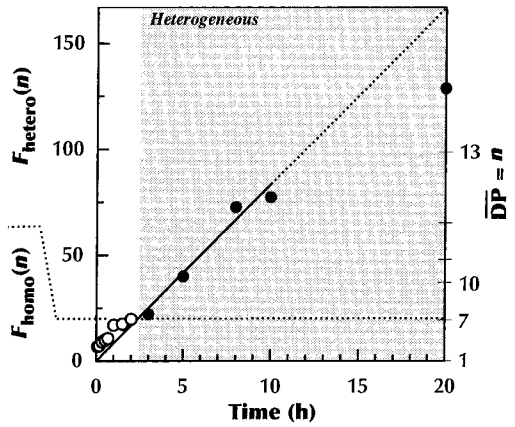

Figure 7. Kinetic plot for the living precipitation polymerization of **1** with MAD (5 mol %) in toluene at 25 °C: homogeneous state (○); heterogeneous state (●). The slope of the diagonal line corresponds to $k_p = 2.32 \times 10^{-3}$ mol^{-1} L s^{-1}.

shown in Figure 6, the increase of [P*(p)], i.e., the decrease of [P*(s)], is almost proportional to n in the range from 7 (completely soluble) to 14 (almost insoluble), and hence [P*(s)] is given by

$$[\mathrm{P^*(s)}] = \frac{14 - n}{14 - 7}[\mathrm{I}]_0 \qquad (2)$$

Equation 3 can be derived from eq 2 and the boundary condition that $k_p t = F_{homo}(7)$ at $n = 7$

$$k_p t = \frac{7}{6[\mathrm{I}]_0}\ln\left(\frac{7 \times (20 - n)}{13 \times (14 - n)}\right) + F_{homo}(7) \equiv F_{hetero}(n) \qquad (3)$$

where $F_{hetero}(n)$ refers to a function of n in a heterogeneous state.

The plots of $F_{homo}(n)$ and $F_{hetero}(n)$ vs polymerization time in Figure 7 fall on a straight line passing through the origin; the slope predicts that $k_p = 2.32 \times 10^{-3}$ mol^{-1} L s^{-1}. For this calculation, data at $\overline{DP}$ (=n) higher than 12.5 were not used in order to exclude logarithmic errors. The time−conversion curve in Figure 4 was calculated with this second-order rate constant and agrees well with the experimental data. It follows from the above kinetic consideration that the precipitating species participate in propagation through a reversible interchange into soluble species.

Scheme 4. Plausible Mechanism for the Cationic Isomerization Ring-Opening Polymerization of 1

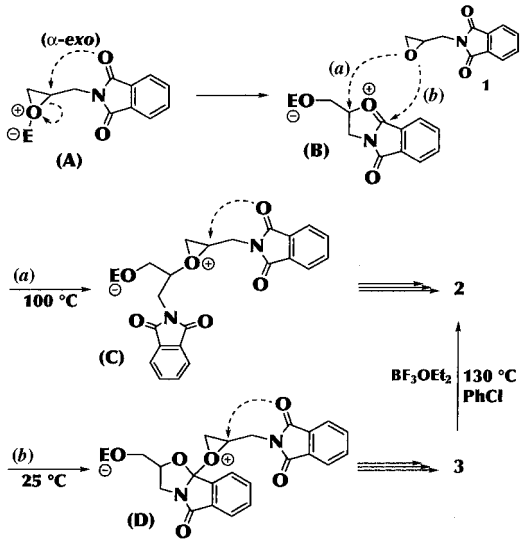

Polymerization Mechanism. A plausible mechanism for the cationic polymerization of **1** is outlined in Scheme 4. The polymerization took place not only with MAD but also with trimethylsilyl trifluoromethanesulfonate or BF_3OEt_2, to give **3** at 0−25 °C and **2** at −30 and more than 100 °C, although MAD yielded no polymer at −30 °C. These observations suggest that oxonium cation **A** activated by coordination of Lewis acid (E) such as MAD would prefer entropically the intramolecular attack of the imide−carbonyl oxygen to the intermolecular addition of **1** (polymerization) at least at more than 0 °C.[8] Furthermore, the α-exo mechanism obeying Baldwin's rule[13] dominates in the above cyclization to give five-membered 4,5-dihydrooxazol-2-ylium cation **B**, as evidenced by the isomerization behavior of **6**, In contrast to six-membered 5,6-dihydro-4*H*-1,3-oxazin-2-ylium cation generated from analogous oxetane imides,[8b] however, it seems to be difficult for **B** to ring-close to a more strained [2.2.1]bicyclic acetal. In addition, all MAD molecules should be completely consumed in the rapid initiation at a very early stage.[11] Therefore, propagation probably involves neither a monomer-activated mechanism[3] nor a monomer-isomerization mechanism.[8] Thus, attack (*b*) of **1** on the cationic carbon of **B** at 25 °C gives **D**, and this step-by-step process continues on the growing end and then affords **3**. At higher temperature, **B** can open by attack (*a*) of **1** on the *O*-methine carbon to afford **2**. However, there is no direct evidence that formation of both polymers are controlled kinetically,[8] although the possibility that **2** is formed according to a usual, straightforward mechanism would be ruled out at high temperature. On the other hand, **2** was also produced in the reaction of **3** with BF_3OEt_2 in PhCl at 130 °C. Again, no depolymerization of **3** was observed in this transformation.[8] This suggests that **3** formed at the beginning of the polymerization could be directly transformed to **2** at high temperature via an acid-catalyzed intermolecular isomerization process with cleavage of acetalic linkage.[14]

The schematic representation of a mechanism for the controlled precipitation polymerization is illustrated in Scheme 5. The solubility equilibrium between soluble and precipitating **3** would play an important role to realize the living nature of polymerization, just as in the well-known cases of chemical equilibria between

Scheme 5

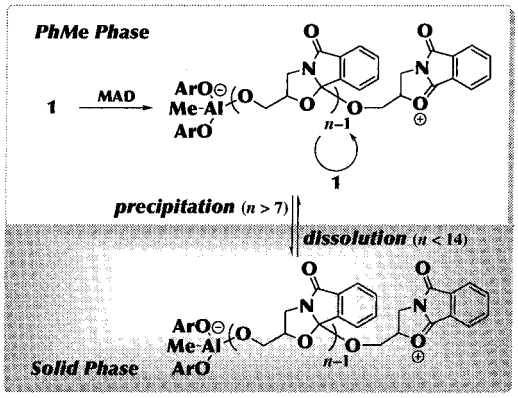

reactive growing ends and dormant covalent species.[1] After living **3** has grown beyond heptamer ($n = 7$) in toluene, it begins to precipitate from the solution. The solubility of a polymer molecule of **3** in toluene tends to decrease with increasing of its $\overline{DP}$. The lower-molecular-weight species in the precipitate, in turn, dissolve and grow again in solution. Consequently, the probably rapid cycle of dissolution and precipitation ensures giving all the growing species practically equal chances of growth to approach uniformity of M_n. The precipitating species may be regarded as a dormant species, in that the living species in the solid phase cannot propagate. The decreased concentration of the soluble species could suppress possible chain-breaking reactions in solution, although we do not have a rational explanation for this. Like **B**, the growing species would have a zwitterionic structure carrying a carbeoxonium reactive end and the other bulky alkoxyaluminate end. By virtue of the sterically hindered silent end, possible ion coupling reactions with each end would be highly restrained not only in solution but also in the solid phase.

As long as the polymerization of **1** is carried out in toluene, the maximum M_n of **3** cannot exceed 2.80×10^3 due to its limited solubility. Up to $M_n = 5.00 \times 10^3$ product was quantitatively yielded by adding dichloromethane to toluene in a 1:4 volume ratio (run no. 8), and the M_n was predictable from the feed ratio of **1** to MAD. This implies that the solubility of the growing species increases with increasing polarity of the medium. However, further addition of dichloromethane made the polymerization system homogeneous and thereby resulted in an uncontrolled polymerization (run no. 9).

Conclusion

We have found that the cationic polymerization of **1** with MAD affords either **2** or **3** depending on temperature. Acetalic linkages in the main chain of **3** are formed in an isomerization ring-opening manner involving the intramolecular nucleophilic attack of the imide−carbonyl group at the growing end. The heterogeneous polymerization in toluene at 25 °C is the first example of a precipitation polymerization to give **3** with nearly uniform chain lengths and a predictable molecular weight from the feed ratio of **1** to MAD. The living nature of polymerization is attained over a very narrow molecular weight range by the physical solubility equilibrium of growing species between solution and precipitates, as in chemical equilibria between reactive growing ends and dormant covalent species.

Supporting Information Available: Text giving detailed kinetic consideration of the precipitation polymerization of **1**. This material is available free of charge via the Internet at http://pubs.acs.org.

References and Notes

(1) For example: (a) Webster, O. W.; Hertler, W. R.; Sogah, D. Y.; Farnham, W. B.; RajanBabu, T. V. *J. Am. Chem. Soc.* **1983**, *105*, 5706. (b) Fayt, R.; Forte, R.; Jacobs, C.; Jérôme, R.; Ouhadi, T.; Teyssié, Ph.; Vershiney, S. K. *Macromolecules* **1987**, *20*, 1442 (c) Webster, O. W. *Science* **1991**, *251*, 887. (d) Sawamoto, M. *Trends Polym. Sci.* **1993**, *1*, 111. (e) Aida, T. *Prog. Polym. Sci.* **1994**, *19*, 469. (f) George, M. K.; Veregin, R. P. N.; Kazmaier, P. M.; Hamer, G. K. *Trends Polym. Sci.* **1994**, *2*, 66. (g) Davis, T. P.; Kukulj, D.; Haddleton, D. M.; Maloney, D. R. *Trends Polym. Sci.* **1995**, *3*, 365. (h) Sawamoto, M.; Kamigaito, M. *Trends Polym. Sci.* **1996**, *4*, 371.

(2) (a) Price, C. C.; Carmelite, D. D. *J. Am. Chem. Soc.* **1956**, *88*, 4039. (b) Aida, T.; Inoue, S. *Macromolecules* **1981**, *14*, 1162. (c) Aida, T.; Inoue, S. *Macromolecules* **1981**, *14*, 1166. (d) Aida, T.; Maekawa, Y.; Asano, S.; Inoue, S. *Macromolecules* **1988**, *21*, 1195. (e) Kuroki, M.; Aida, T.; Inoue, S. *Makromol. Chem.* **1988**, *189*, 1305. (f) Watanabe, Y.; Aida, T.; Inoue, S. *Macromolecules* **1990**, *23*, 2612.

(3) (a) Penczek, S.; Kubisa, P.; Szymanski, R. *Macromol. Chem., Macromol. Symp.* **1986**, *3*, 203. (b) Wojtania, M.; Kubisa, P.; Penczek, S. *Macromol. Chem., Macromol. Symp.* **1986**, *6*, 201. (c) Biedron, T.; Kubisa, P.; Penczek, S. *J. Polym. Sci., Part A: Polym. Chem.* **1991**, *29*, 619.

(4) Takeuchi, D.; Aida, T. *Macromolecules* **1996**, *29*, 8096.

(5) Hayashi, Y.; Kayatani, T.; Sugimoto, H.; Suzuki, M.; Inomata, K.; Uehara, A.; Mizutani, Y.; Kitagawa, T.; Maeda, Y. *J. Am. Chem. Soc.* **1995**, *117*, 11220.

(6) Saegusa, T.; Matsumoto, S. *J. Polym. Sci., Part A-1* **1968**, *6*, 1559.

(7) Peaks at $203 \times n$ mass units are assignable to the parent polymer − 18 (H_2O) ions, while those at $203 \times n - 44$ mass units might be generated via additional fragmentation of a molecule of acetaldehyde (MW = 44). These ion peaks appeared at substantially low mass units compared with the M_n estimated by SEC based on polystyrene calibration, presumably because of main chain scission under the ionization conditions applied.

(8) (a) Kanoh, S.; Nishimura, T.; Senda, H.; Ogawa, H.; Motoi, M.; Tanaka, T.; Kano, K. *Macromolecules* **1999**, *32*, 2438. (b) Kanoh S.; Nishimura T.; Tsuchida T.; Senda H.; Motoi M.; Takani M.; Matsuura N. *Macromol. Chem. Phys.* **2001**, *202*, 2489.

(9) Nishimura, T.; Kanoh, S.; Senda, H.; Tanaka, T.; Ando, K.; Ogawa, H.; Motoi, M. *J. Chem. Soc.*; *Chem. Commun.* **1998**, *43* 1998.

(10) When a small amount of toluene contained in the curds of precipitates was removed by vacuum evaporation, the resulting precipitates were incapable of polymerizing **1** in toluene. In contrast, the homogeneous polymerization in a 1:1 mixture of toluene and CH_2Cl_2 was successful with the solvent-free precipitates. However, the control of molecular weight resulted in failure, as in the homogeneous polymerization of run no. 9 in Table 1.

(11) ^1H NMR trace of the polymerization in toluene-d_8 showed that the initiation was completed within a few minutes; see ref 8b.

(12) See Supporting Information.

(13) Baldwin, J. E. *J. Chem. Soc., Chem. Commun.* **1976**, 734.

(14) Chikaoka, S.; Takata, T.; Endo, T. *Macromolecules* **1992**, *25*, 625.

MA010577G